Spin liquid state in a rare-earth hyperkagome lattice

J. Khatua,[1] S. Bhattacharya,[2] Q. P. Ding,[3] S. Vrtnik,[4] A. M. Strydom,[5] N. P. Butch,[6] H. Luetkens,[7] E. Kermarrec,[2] M. S. Ramachandra Rao,[8,9] A. Zorko,[4,10] Y. Furukawa,[3] and P. Khuntia[1,9,11,*]

[1]*Department of Physics, Indian Institute of Technology Madras, Chennai 600036, India*
[2]*Université Paris-Saclay, CNRS, Laboratoire de Physique des Solides, 91405 Orsay, France*
[3]*Ames Laboratory, U.S. DOE, and Department of Physics and Astronomy, Iowa State University, Ames, Iowa 50011, USA*
[4]*Jožef Stefan Institute, Jamova c. 39, 1000 Ljubljana, Slovenia*
[5]*Highly Correlated Matter Research Group, Department of Physics, University of Johannesburg, PO Box 524, Auckland Park 2006, South Africa*
[6]*NIST Center for Neutron Research, National Institute of Standards and Technology, Gaithersburg, Maryland 20899, USA*
[7]*Laboratory for Muon-Spin Spectroscopy, Paul Scherrer Institute, CH-5232 Villigen-PSI, Switzerland*
[8]*Department of Physics, Nano Functional Materials Technology Centre and Materials Science Research Centre, Indian Institute of Technology Madras, Chennai-600036, India*
[9]*Quantum Centre for Diamond and Emergent Materials, Indian Institute of Technology Madras, Chennai 600036, India*
[10]*Faculty of Mathematics and Physics, University of Ljubljana, Jadranska u. 19, 1000 Ljubljana, Slovenia*
[11]*Functional Oxide Research Group, Indian Institute of Technology Madras, Chennai 600036, India*

(Received 27 April 2022; revised 16 August 2022; accepted 26 August 2022; published 6 September 2022)

Quantum fluctuations enhanced by frustration and subtle interplay between competing degrees of freedom offer an ideal ground to realize novel states with fractional quantum numbers in quantum materials that defy standard theoretical paradigms. Quantum spin liquid (QSL) is a highly entangled state wherein frustration-induced strong quantum fluctuations preclude symmetry-breaking phase transitions down to zero temperature without any order parameter. Experimental realizations of QSL in quantum materials with spin dimensionality greater than one is very rare. Here, we present our thermodynamic, nuclear magnetic resonance, muon spin relaxation, and inelastic neutron scattering studies of a rare-earth hyperkagome compound $Li_3Yb_3Te_2O_{12}$ in which Yb^{3+} ions constitute a three-dimensional spin lattice without any detectable disorder. Our comprehensive experiments evince neither signature of magnetic ordering nor spin freezing down to 38 mK that suggest the realization of dynamic liquid-like ground state in this antiferromagnet. The ground state of this material is interpreted by a low energy $J_{\text{eff}} = 1/2$ degrees of freedom with short-range spin correlations. The present results demonstrate a viable basis to explore spin-orbit driven enigmatic correlated quantum states in a class of rare-earth-based three-dimensional frustrated magnets that may open avenues in theoretical and experimental search for spin liquids.

DOI: 10.1103/PhysRevB.106.104404

I. INTRODUCTION

Quantum materials wherein superposition and entanglement are at play may exhibit exotic physical phenomena, such as spin liquids with fractional quantum numbers coupled to emergent gauge fields that offer an exciting paradigm in advancing quantum science and technology [1–4]. The experimental realization of quantum spin liquid (QSL) with exotic collective excitations in quantum materials sets an outstanding track in modern condensed matter since the seminal proposal of P. W. Anderson in 1973 [5,6]. QSLs are characterized by the absence of magnetic order down to $T = 0$, long-range entanglement, coherent fluctuation of spins, and the preservation of local symmetries despite strong exchange interaction between spins [6–9]. Fractionalization of quantum numbers is a fingerprint of QSLs which is different from spin waves in conventional magnets. This is a well-established scenario in one-dimensional (1D) magnets. It has been suggested that also 2D and 3D QSLs can host fractionalized deconfined quasiparticles such as spinons and Majorana fermions, the understanding of which is essential in advancing fundamental physics and is highly relevant for fault-tolerant quantum computing [6,10–17]. However, the presence of perturbations, such as extra exchange couplings, unavoidable disorder, and defects in real materials put a strong constraint for the ideal realization of QSLs with $D \geqslant 2$ [18–20].

Moreover, 3D spin lattices that are composed of small triangular motifs in an edge- or corner-sharing fashion can host strong frustration similar to 2D spin lattices, namely, quantum fluctuations in such 3D frustrated lattices with low values of spin could lead to unconventional ground states including spin liquids [11,12]. This has motivated us to explore quantum materials with a rich potential to host such states with fractional quantum numbers [21–23]. The intertwining of spin-orbit coupling, anisotropy, spin correlations and frustration in rare-earth magnets offers another route to realize unique quantum states [4,7,24–26]. In recent years, spin-orbit-driven frustrated magnets have provided a viable ground to realize emergent quantum phenomena ranging from

*pkhuntia@iitm.ac.in

spin ice states [7,27] to spin liquid [15,24,28] and anomalous and spontaneous Hall effects [29,30] to Bose-Einstein condensate phases [25,31]. In lanthanide magnetic materials, the interplay between spin-orbit coupling and low-symmetry crystal electric field leads to Kramers doublets where effective $J_{\text{eff}} = 1/2$ moments of rare-earth ions appear, contrary to pure $S = 1/2$ moments in transition-metal ions. The 3D spin-lattice-based quantum magnets host a plethora of interesting ground state properties including nontrivial short-range spin correlations [32], unconventional spin glass [33], and magnetic Coulomb phases [34,35]. For example, the lanthanide family $A_2B_2O_7$ where rare-earth ions form a pyrochlore lattice is a rich reservoir that hosts a wide range of quantum phenomena owing to the complex interplay between competing degrees of freedom [7,36]. Quite recently, $Ce_2Zr_2O_7$ was proposed to be a 3D QSL candidate, where Ce^{3+} ions with $J_{\text{eff}} = 1/2$ moments decorate a network of corner-sharing tetrahedra [37,38]. The observation of $U(1)$ QSL and emergent excitations driven by multipolar interactions in its Sn analog $Ce_2Sn_2O_7$ also set a unique example of a 3D spin lattice for exploring quantum many-body phenomena [39]. Furthermore, the garnet series $R_3B_5O_{12}$ (R = rare-earth ions and B = Ga and Al) where the rare-earth ions decorate two interpenetrating hyperkagome lattices are known to harbor myriads of interesting quantum phenomena such as long-range multipolar states [40,41] and Ising antiferromagnets [42,43]. However, most of the garnets undergo a magnetic phase transition at lower temperature [44–50]. Therefore, the search for an ideal 3D spin lattice to realize a QSL state poses a particularly challenging problem. For example, no report has been published so far on a structurally perfect $4f$-based hyperkagome lattice in which high degree of spin frustration and anisotropic interactions mediated by spin-orbit coupling could stabilize an ideal 3D spin liquid.

Here, we report a rare-earth based quantum magnet $Li_3Yb_3Te_2O_{12}$ and investigate its inherent physics of 3D frustrated spin-lattice with $J_{\text{eff}} = 1/2$ moments of Yb^{3+} ions. $Li_3Yb_3Te_2O_{12}$ crystallizes in the cubic space group $Ia\bar{3}d$, where Yb^{3+} ions form two interpenetrating hyperkagome spin lattices. Our thermodynamic results suggest the presence of a Kramers doublet state and antiferromagnetic interaction between $J_{\text{eff}} = 1/2$ spins at low temperature. The absence of long-range magnetic ordering and spin freezing down to at least 38 mK in our ac susceptibility, specific heat, and NMR experiments is the first fingerprint of a spin liquid state in this frustrated quantum material. Furthermore, specific heat measurements show the presence of short-range spin correlations in this antiferromagnet. Our complementary experimental probes thus demonstrate a dynamic ground state and a field-induced gapped behavior in the spin excitation spectrum in this spin-orbit-driven frustrated hyperkagome quantum material.

II. METHODS

A. Sample synthesis

Polycrystalline samples of $Li_3Yb_3Te_2O_{12}$ (henceforth LYTO) were synthesized by a standard solid-state reaction of Li_2CO_3 (99.0%, Alfa Aesar), Yb_2O_3 (99.998%, Alfa Aesar), and TeO_2 (99.9995%, Alfa Aesar) [51]. Since the lanthanide oxide and Li_2CO_3 are generally hygroscopic, before being weighted, Yb_2O_3 and Li_2CO_3 were preheated at 900 °C and 100 °C, respectively. The stoichiometric mixtures of starting materials were pelletized and heated at 800 °C for 30 h in air with several intermittent grindings. We also used Y_2O_3 (99.999%, Alfa Aesar) and followed the same procedure to prepare the isostructural nonmagnetic analog $Li_3Y_3Te_2O_{12}$. The phase purity was checked by room temperature powder x-ray diffraction (XRD) using smartLAB Rigaku x-ray diffractometer equipped with Cu Kα radiation ($\lambda = 1.54$ Å). The crystal structure of LYTO was confirmed by the Rietveld refinement of x-ray diffraction data using GSAS software [52]. All the XRD peaks could be indexed with the cubic space group $Ia\bar{3}d$ and lattice parameter $a = 12.173$ Å [51]. No secondary phase is detected in XRD. The Rietveld refinement of XRD data rules out the presence of any intersite disorder between the constituent atoms. The observed sharp XRD peaks indicate high-quality polycrystalline samples of LYTO investigated in this paper.

B. Magnetization measurements

Magnetization data were acquired using a Quantum Design SQUID magnetometer in the temperature range 2 K $\leqslant T \leqslant$ 350 K. Magnetic susceptibility [$\chi(T)$] data were recorded in magnetic fields 0.1 and 1 T and the zero-field cooled (ZFC) and field cooled (FC) data were collected in a magnetic field of 0.01 T. To determine the effective magnetic moment (μ_{eff}) and Curie-Weiss (CW) temperature (θ_{CW}), the high-temperature (> 160 K) inverse susceptibility ($1/\chi(T)$) data were fitted with the CW law, $\chi = \chi_0 + C/(T - \theta_{\text{CW}})$. Here C is the Curie constant which is used to calculate $\mu_{\text{eff}} = \sqrt{8C}\ \mu_B$, χ_0 is the temperature-independent paramagnetic susceptibility, and θ_{CW} provides an estimate of the magnetic exchange interactions. The isothermal magnetization [53] follows $M/M_s = B_{1/2}\ (y)$, where $B_J(y) = [\frac{2J+1}{2J}\coth[\frac{y(2J+1)}{2J}] - \frac{1}{2J}\coth\frac{y}{2J}]$ is the Brillouin function, $M_s\ (= gJ\mu_B)$ is the saturation magnetization, and $y = g\mu_B J\mu_0 H/k_B T$, where μ_B is the Bohr magneton, g is the Landé g factor. The Brillouin function fit with fixed $J = 1/2$ to magnetization data yields Landé g factor, $g = 3.54 \pm 0.02$.

C. Specific heat measurements

Specific heat measurements were performed in the temperature range 0.35 K $\leqslant T \leqslant$ 270 K under magnetic fields 0 T $\leqslant \mu_0 H \leqslant$ 7 T, using a thermal-relaxation technique provided by Quantum Design, PPMS. Furthermore, specific heat measurements were carried out separately in the temperature range 0.054 K $\leqslant T \leqslant$ 4 K in zero field (ZF) using a dilution refrigerator which was also used to measure ac susceptibility in the temperature range 0.045 K $\leqslant T \leqslant$ 4 K at six different frequencies using a Dynacool PPMS instrument from Quantum Design. The total specific heat of LYTO can be expressed as a sum of contributions from the electronic spins in the ground-state Kramers doublet (C_{mag}), lattice contribution (C_{lat}) and nuclear contribution (C_n) i.e., $C_{\text{tot}}(T) = C_{\text{mag}}(T) + C_{\text{lat}}(T) + C_n$. We also measured specific heat of the $Li_3Y_3Te_2O_{12}$ which we used as a nonmagnetic analog to subtract the lattice contribution. The magnetic specific heat

was obtained after subtracting the lattice and nuclear Schottky $C_n \propto T^{-2}$ contributions.

D. NMR measurements

Field-swept ^{7}Li ($I = 3/2$, and gyromagnetic ratio 16.54 MHz/T) NMR measurements down to 38 mK at several frequencies were carried out on a homemade phase-coherent spin-echo pulse spectrometer equipped with a 9 T Oxford magnet. The low-temperature NMR measurements were performed with an Oxford Kelvinox dilution refrigerator. NMR spectra measurements were carried out using a standard Han-echo sequence while the spin-lattice relaxation time measurements were performed following saturation-recovery method. In LYTO, ^{7}Li is an NMR active nucleus which couples with Yb^{3+} spins via hyperfine interaction. Therefore, ^{7}Li NMR can probe the intrinsic magnetic susceptibility as well as low-energy spin excitations via NMR shift and spin-lattice relaxation, respectively. The temperature dependence of the NMR shift (K) at different frequencies was extracted from the fit of the field-swept NMR spectra. For an anisotropic magnetic material, three different components of NMR shift $K(T)$ such as $K_{\rm iso}$ (isotropic shift), $K_{\rm ax}$ (axial shift), and $K_{\rm aniso}$ (anisotropic shift), arising from a general hyperfine coupling tensor, can be determined from the observed experimental line shape. In this respect, the principal components $K_{\rm X}$, $K_{\rm Y}$, and $K_{\rm Z}$ of tensor $K(T)$ can be used to define $K_{\rm iso} = 1/3(K_{\rm X} + K_{\rm Y} + K_{\rm Z})$, $K_{\rm aniso} = 1/2(K_{\rm Y} - K_{\rm X})$, and $K_{\rm ax} = 1/6(2K_{\rm Z} - K_{\rm X} - K_{\rm Y})$ [54,55]. The temperature dependence of the NMR shift scales with the magnetic susceptibility as $K_{\rm ax/iso}(T) = K_0 + (A_{\rm hf}^{\rm ax/iso}/N_{\rm A}\mu_{\rm B})\chi_{\rm spin}(T)$, where K_0 accounts for the temperature-independent chemical and orbital shift, $A_{\rm hf}$ is the hyperfine coupling constant between ^{7}Li nucleus and Yb^{3+} spins, $\mu_{\rm B}$ is the Bohr magneton and $N_{\rm A}$ is the Avogadro number, respectively. To extract the hyperfine couplings, the standard Clogston-Jaccarino plot (see Supplemental Material (SM) Fig. 7 [53]) was used to extract hyperfine coupling constants in two temperature regimes and the obtained fitting parameters are given in SM note 5. The fit of NMR spectra below 1 K is not very good (see SM Fig. 6), which could be due to an additional spectral weight in the low-field side at low temperature, however, the origin is not clear at this moment. To uncover the low-energy dynamics of Yb^{3+} spins in LYTO, we conducted spin-lattice relaxation time measurement. To estimate T_1^{-1}, the recovery of longitudinal nuclear magnetization data were fitted by the single exponential function $M_z(t) = (M_0 - M(t))/M_0 = A \exp(-t/T_1)$ in the entire temperature range of the investigation, where M_0 is the equilibrium magnetization, $M_z(t)$ is the magnetization at time t after the saturation pulse, and A is a constant. The validity of a single exponential function in a wide temperature range suggests that the electronic moments are uniformly distributed in the host lattice without disorder. The fit of the recovery curves with the standard expression relevant for $I = 3/2$ nucleus was not as good as the single exponential function.

E. Muon spin relaxation (μSR)

Muon spin relaxation measurements were performed at the Paul Scherrer Institute on the GPS instrument. A weak transverse field of 50 Oe was applied to determine the initial asymmetry parameter. ZF and longitudinal applied fields (LF) data sets were obtained using VETO mode resulting in minimal background signal (<0.02).

F. Inelastic neutron scattering

Time-of-flight inelastic neutron scattering measurements were carried out at the NIST Center for Neutron Research (NCNR, Gaithersburg, MD) on the DCS spectrometer. To isolate the field evolution of the inelastic spectrum, a field-independent background, made of the average of the 0 and 2 T data sets for $E > 0.85$ meV and of the average of the 7, 8, 9, and 10 T data sets for $E < 0.85$ meV was subtracted from the Q-integrated energy cuts. Simulations of powder-averaged dynamical structure factor for inelastic neutron scattering were done with the SpinW software [56].

III. RESULTS

A. Magnetization

The magnetic susceptibility $\chi(T)$ data do not exhibit any signs of a magnetic phase transition down to 2 K [Fig. 1(c)]. The CW fit to the high-temperature (> 160 K) $\chi(T)$ data yields $\theta_{\rm CW} \approx -78$ (1) K, $\mu_{\rm eff} = 4.4\ \mu_{\rm B}$, which is close to $\mu_{\rm eff} = 4.54\ \mu_{\rm B}$ of a free Yb^{3+} ($J = 7/2$) spin and $\chi_0 = 4.97 \times 10^{-4}$ cm^3/mol. The estimated large negative $\theta_{\rm CW}$ is ascribed to the energy scale of excited crystal electric-field levels [24]. The interaction energy scale of $4f$ systems is much lower and is in our case revealed at low-temperature where the CW fit of $1/\chi(T)$ data in the temperature range $2\ {\rm K} \leqslant T \leqslant 10$ K yields $\mu_{\rm eff} = 3.0\ \mu_{\rm B}$ and $\theta_{\rm CW} \approx -0.3$ K $\pm$ 0.03 K. The obtained effective moment is smaller than the Yb^{3+} free-ion value, which suggests the formation of a Kramers doublet state at low temperature, as also confirmed by specific heat measurements (see next section). The small and negative CW temperature indicates the presence of a weak antiferromagnetic interaction between the pseudo 1/2 moment of Yb^{3+} ions with approximate interaction energy of the order of $\theta_{\rm CW}$. The absence of long-range magnetic order down to 38 mK in our NMR experiment (discussed later) suggests that the present hyperkagome is a frustrated lattice with the frustration parameter $f = |\theta_{\rm CW}|/T_{\rm min} \sim 8$, which suggests that LYTO is a highly frustrated magnet. The CW temperature of most $4f$ systems is typically small and thus the onset of spin correlations develops at very low temperature in these quantum materials [37,39,43,57,58]. Furthermore, the absence of any bifurcation in ZFC and FC susceptibility data (see SM Fig. 2 [53]) in an applied magnetic field of 100 Oe suggests that Yb^{3+} spins are not frozen down to 2 K. To confirm the absence of spin freezing, we performed ac susceptibility measurements down to millikelvin temperatures at different frequencies. Figure 1(d) depicts the real part of the ac susceptibility as a function of temperature down to 45 mK and it exhibits a broad maximum around 80 mK, which suggests the persistence of short-range interaction between Yb^{3+} moments in LYTO [59–61]. Importantly, the absence of any frequency dependency of ac susceptibility strongly rules out glassy behavior of Yb^{3+} spins in LYTO. The magnetization isotherms at a few selected temperatures are shown

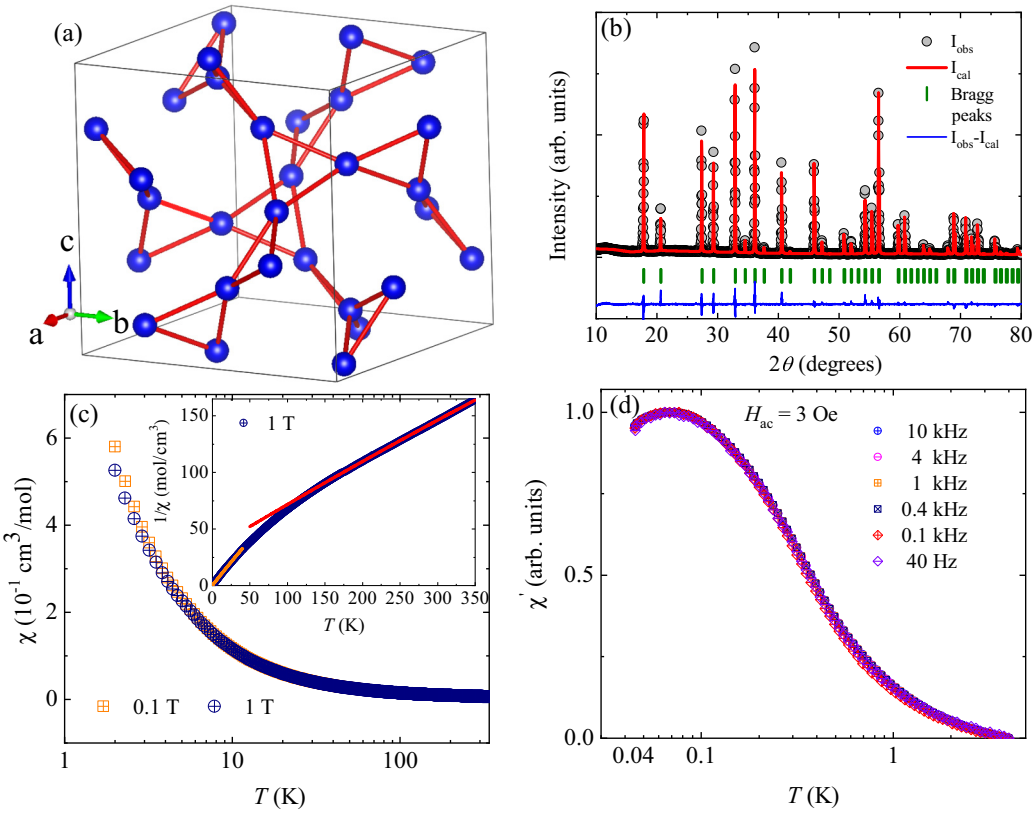

FIG. 1. Crystal structure and bulk magnetic properties of LYTO. (a) The position of the Yb^{3+} magnetic ions within the unit cell. These Yb^{3+} ions decorate two interpenetrating chains of 3D corner-shared triangles known as the hyperkagome lattice. (b) Rietveld refinement of powder x-ray diffraction data recorded at room temperature. The experimentally observed points (circles), the calculated Rietveld refinement profile (solid line), the Bragg reflection positions (olive vertical bars), and the difference between the observed and calculated intensity (blue line) are shown. (c) The temperature dependence of magnetic susceptibility in two magnetic fields. The inset shows the temperature-dependent inverse magnetic susceptibility data with the orange and red lines showing the Curie-Weiss fits for the low- and high-temperature data, respectively. (d) The temperature dependence of the real part of ac susceptibility at different frequencies down to 45 mK.

in SM Fig. 3 and the absence of any visible hysteresis rules out the presence of any ferromagnetic signal. The calculated Landé g factor, $g = 3.46 \pm 0.02$, from the low-temperature CW fit of magnetic susceptibility, is close to that obtained from the Brillouin function fit of the magnetization isotherm. A similar value of powder average of Landé g factor is also observed in Yb-based 3D pyrochlore systems, suggesting the single-ion properties of LYTO are expected to be similar to the pyrochlore material [60].

B. Specific heat

Specific heat is an excellent probe to reveal the nature of ground-state and spin correlations in quantum materials. Figure 2(a) shows the total specific heat measured in zero-magnetic field. The absence of any λ-type peak suggests that there is no phase transition down to 54 mK. After subtracting the lattice contribution using the nonmagnetic analog $Li_3Y_3Te_2O_{12}$ and the nuclear contribution associated with the hyperfine splitting of the Yb^{3+} nuclear spin multiplet [62], the resulting temperature dependence of magnetic specific heat, $C_{mag}(T)$ is shown in Fig. 2(b) in the temperature range 54 mK $\leqslant T \leqslant$ 10 K. Below 2 K, the ZF magnetic specific heat, $C_{mag}(T)$, starts increasing and shows a broad maximum around 0.18 K, which indicates the presence of short-range spin correlations between Yb^{3+} moments [28]. The presence of broad maximum around 0.18 K agrees well with the estimated CW temperature at low temperatures and it is consistent with general expectation for a QSL candidate [60].

In finite applied magnetic fields, it is observed that the broad maximum shifts to higher temperatures with increased field, which opens a gap owing to the Zeeman splitting of the lowest Kramers doublet state. It is worth noting that we have not observed any suppression of $C_{mag}(T)$ in the presence of magnetic field, thus ruling out the presence of disorder [63]. Therefore, there are no uncertainties in Schottky contribution due to the effect of disorder in the extracted $C_{mag}(T)$ data. It is observed that the gap size increases upon increasing magnetic fields (see SM Figs. 4 and 9). The fit of the field dependence of gap yields $g = 3.34 \pm 0.01$, which is consistent with that obtained from the magnetization measurements. The magnetic-field-induced Zeeman gap in magnetic specific heat data is observed at very low temperature in several rare-earth-based spin-liquid candidates with relatively small exchange interactions compared to the Zeeman splitting [37,63].

In Fig. 2(c), we present the estimated entropy change, ΔS, by integrating $C_{mag}(T)/T$ data in the temperature range 0.054 K $\leqslant T \leqslant$ 16 K and 0.35 K $\leqslant T \leqslant$ 16 K for ZF and

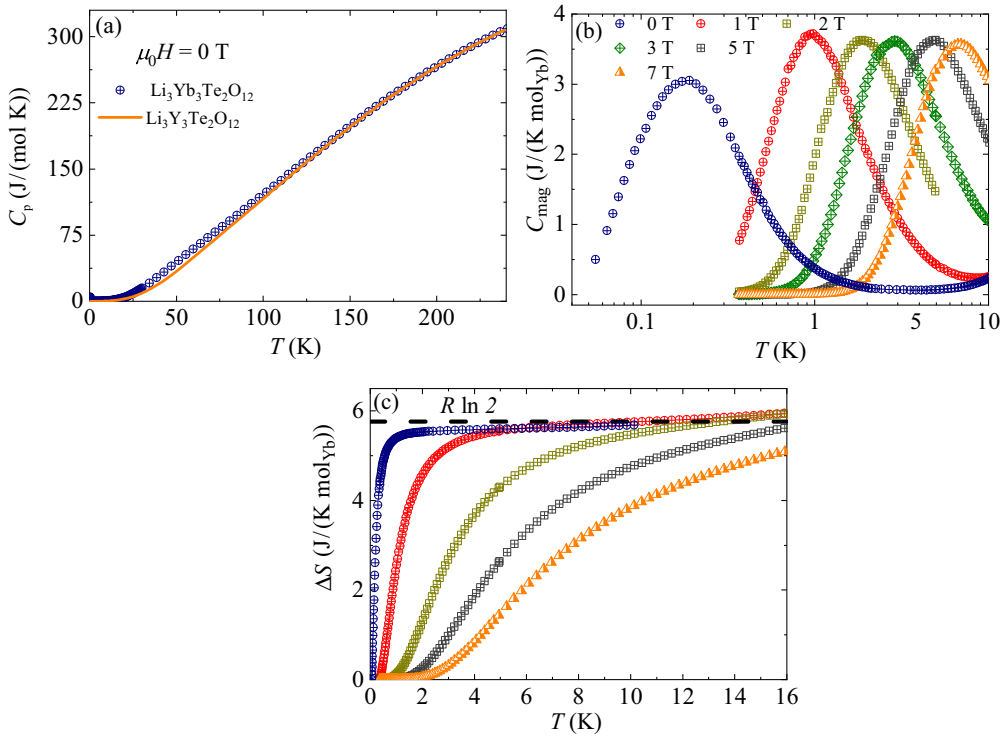

FIG. 2. Specific heat of LYTO in various magnetic fields. (a) The temperature dependence of specific heat (C_p) of LYTO and its nonmagnetic analog $Li_3Y_3Te_2O_{12}$ in zero-magnetic field. (b) Low-temperature magnetic specific heat [$C_{mag}(T)$] after subtraction of lattice and nuclear contributions in zero field as well as nonzero field. (c) The temperature dependence of entropy change [$\Delta S = \int C_{mag}(T)/T\, dT$, the temperatures of the color plots correspond to those in (b)] for magnetic fields up to 7 T with the expected entropy (R ln 2 for spin-1/2) indicated by a black dashed line.

finite magnetic fields, respectively. The total entropy (Rln2) expected for $J_{eff} = 1/2$ state is fully recovered for ZF as well as for nonzero magnetic fields. This provides the concrete evidence of a Kramers doublet ground state of Yb^{3+} spins in LYTO at low temperature.

C. Muon spin relaxation

We also performed muon spin relaxation (μSR), to confirm the absence of static magnetism on a microscopic scale. With its spin $I = 1/2$ and gyromagnetic ratio $\gamma_\mu/2\pi = 135.5$ MHz/T, an implanted muon is an unbeatably sensitive probe of magnetism. Figure 3 shows the muon asymmetry obtained in ZF and LF applied field configurations down to 1.57 K. The ZF relaxation shape is nearly exponential in the T range 1.57–50 K. A fit of the asymmetry using a stretched exponential function $A(t) = e^{-(\lambda t)^\beta}$ leads to large $\beta \sim 0.8 - 1$ values. This is typical of strongly fluctuating local fields and, indeed, relaxation under LF remains almost unchanged, except for the highest field of 7500 Oe, corroborating the dynamical character of Yb^{3+} moments. We further investigated this dynamics through temperature dependence of the muon spin relaxation rate λ (Fig. 3). Above 20 K, the strong relaxation ($\sim$1.85 μs^{-1}) is typical of other related $4f$ rare-earth-based magnetic materials, such as $Yb_3Ga_5O_{12}$ or $Yb_2Ti_2O_7$, and is consistent with fast fluctuations assuming a similar local field amplitude [32]. The slight decrease of λ at low temperatures can be understood in the context of the presence of antiferromagnetic spin correlations, and the first-order $1/T$-expansion $\lambda(T) = \lambda^{(\infty)}(1 + \theta_{CW}/T)$ [64] gives a crude estimate of $\theta_{CW} = -0.25(5)$ K [the red line in Fig. 3(c)], in agreement with magnetization measurements.

D. Nuclear magnetic resonance

Nuclear magnetic resonance is a unique microscopic probe employed to shed insight into the ground state, intrinsic magnetic susceptibility, and low-energy excitations in this material. We carried out NMR experiments in LYTO to confirm the absence of magnetic ordering down to the lowest experimentally accessible temperatures and to track static and dynamic susceptibilities. ^{7}Li NMR spectra are relatively narrow at room temperature (see SM Fig. 5), however, they exhibit a marked broadening below 10 K due to the presence of anisotropic interactions and the development of Yb^{3+} electron spin correlations at low temperature. We observed no detectable line corresponding to the satellite transitions on both sides of the central transition, which indicates the presence of a very weak quadrupole interaction. Furthermore, the line shape was found asymmetric, indicating the presence of either asymmetry in the hyperfine coupling between the Li nucleus and Yb^{3+} spins or asymmetry in spin susceptibility at low temperature, both leading to asymmetry in hyperfine fields. The smooth evolution of the NMR spectra in the entire temperature range rules out the presence of a long-range magnetic ordering at least down to 38 mK. The observation

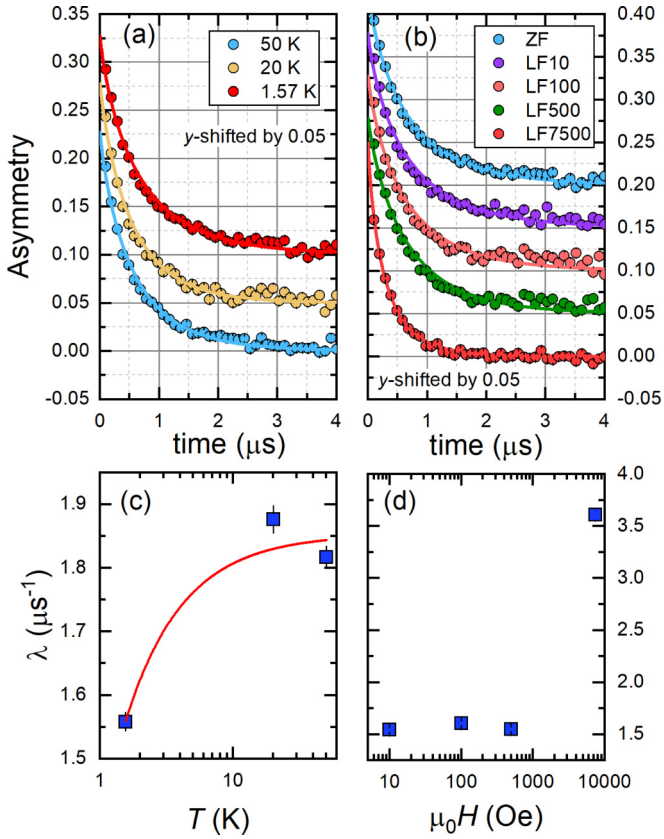

FIG. 3. μSR data confirming a dynamic ground state in LYTO. Muon asymmetry decay obtained in ZF (a) and various LFs at 1.57 K (b) (symbols). The data sets have been shifted vertically by 0.05 for clarity. Lines are fits to a stretched exponential function (see text). The temperature (c) and longitudinal-field (d) dependence of the muon spin relaxation rate λ extracted, respectively, from (a) and (b). The red line shows the $1/T$ expansion of $\lambda(T)$ and indicates the presence of antiferromagnetic spin correlations (see text). Error bars depict an uncertainty of one standard deviation.

of a clear shift of spectra in Fig. 4(a) uniquely determines the intrinsic uniform static spin susceptibility on a microscopic scale. It is independent and saturates to a finite value in the low-temperature limit due to the strong polarization of the Yb^{3+} moments under the applied magnetic field.

Figure 4(b) presents the temperature dependence of the isotropic NMR shift, K_{iso}, and the axial shift K_{ax}, that were extracted from the fitting of NMR spectra. At high-temperatures, both K_{iso} and K_{ax} scale with bulk magnetic susceptibility as expected due to significant hyperfine coupling between ^{7}Li nucleus and Yb atom (see SM Fig. 7 [53]). The scaling of K with χ indicates that the macroscopic magnetization is intrinsic and originates from Yb^{3+} electronic moments. The NMR shift reveals the presence of an anisotropic hyperfine field as expected for $4f$ quantum magnets possibly associated with spin-orbit interactions.

The nuclear spin-lattice relaxation rate (T_1^{-1}) probes the wave-vector q-averaged low-energy spin excitations owing to dynamical electron spin susceptibility in the ground state of correlated quantum materials. Figure 4(c) shows the temperature dependence of T_1^{-1} in three different magnetic fields, which exhibits the presence of three different relaxation regimes. Upon lowering the temperature from 300 K, T_1^{-1} increases in the intermediate temperature range and exhibits a plateau around 70 K. Such increase of T_1^{-1} is not expected for paramagnetic Yb^{3+} spins but is rather due to crystal electric field effects, where spin fluctuations ν slow down upon decreasing temperature leading to the enhancement of NMR relaxation rate in the fast fluctuation regime, where $1/T_1 \propto 1/\nu$ [65]. Below 70 K, T_1^{-1} remains constant and field-independent down to 10 K, which suggests that the relaxation is dominated by paramagnetic fluctuations of Yb^{3+} spins. At low T, i.e., below $\sim$ 10 K, depending on the field, a dramatic field dependence of T_1^{-1} develops with a decrease of the T_1^{-1} value larger than two orders of magnitude in 4.8 T compared to that in 1.24 T at 1.6 K. The relaxation rate, T_1^{-1} decreases exponentially in the temperature range 0.2 K $\leqslant T \leqslant$ 10 K, suggesting a gapped excitation spectrum. It is also observed that T_1^{-1} drops faster in higher magnetic fields which again suggests a field-driven gap as the specific heat data does. In Fig. 4(d), we present T_1^{-1} as a function of inverse temperature (T^{-1}) in a semilog plot where the phenomenological model relevant for thermally activated behavior, i.e., $T_1^{-1} \propto \exp(-\Delta/k_B T)$ yields a straight line with a slope proportional to the gap [65,66]. The obtained gap indeed scales linearly with the applied magnetic field (see SM Fig. 9), which is consistent with the specific heat results. In addition, three distinct energy regimes are also observed in the spin-spin relaxation rate (T_2^{-1}; see SM Fig. 8 [53]). The absence of any peak feature in the temperature dependence of T_1^{-1} rules out the presence of any phase transition also from the spin dynamics perspective down to 200 mK, the lowest temperature that was reached in our spin-lattice relaxation experiment. NMR results thus reveal the presence of a dynamic ground state down to 38 mK with a field-induced gap owing to Zeeman splittings of the Kramers doublet state.

E. Inelastic neutron scattering

To investigate in more detail the nature of excitations at low energy, we carried out inelastic neutron scattering measurements on the cold neutron time-of-flight instrument (DCS) at the NCNR (Gaithersburg, MD). Figure 5 shows the dynamical structure factor measured for an incident energy $E_i = 3.27$ meV with a resolution of 0.11 meV (FWHM). The inelastic spectrum of the ZF data set is essentially featureless [Fig. 5(a)]. The Q-integrated energy cut [Fig. 5(e)] can be well fitted to an elastic Gaussian line plus a quasielastic Lorentzian profile, $S(Q,E) \sim (1 - e^{-E/k_B T})^{-1} E\Gamma/(E^2 + \Gamma^2)$, accounting for the magnetic contribution. In agreement with the NMR and μSR results, the Yb^{3+} ions are found to be in a paramagnetic fluctuating regime characterized by a quasielastic line with the linewidth $\Gamma = 0.05(2)$ meV setting an upper value of the energy scale of the interactions ($\sim$0.6 K), which is consistent with all other results. Upon increasing the field, a nondispersive mode emerges from the elastic line [Figs. 5(b)–5(d)] whose median position depends linearly on the applied field [Fig. 5(g)]. It is ascribed to the Zeeman splitting of the effective spin $J_{eff} = 1/2$ of the Kramers doublet.

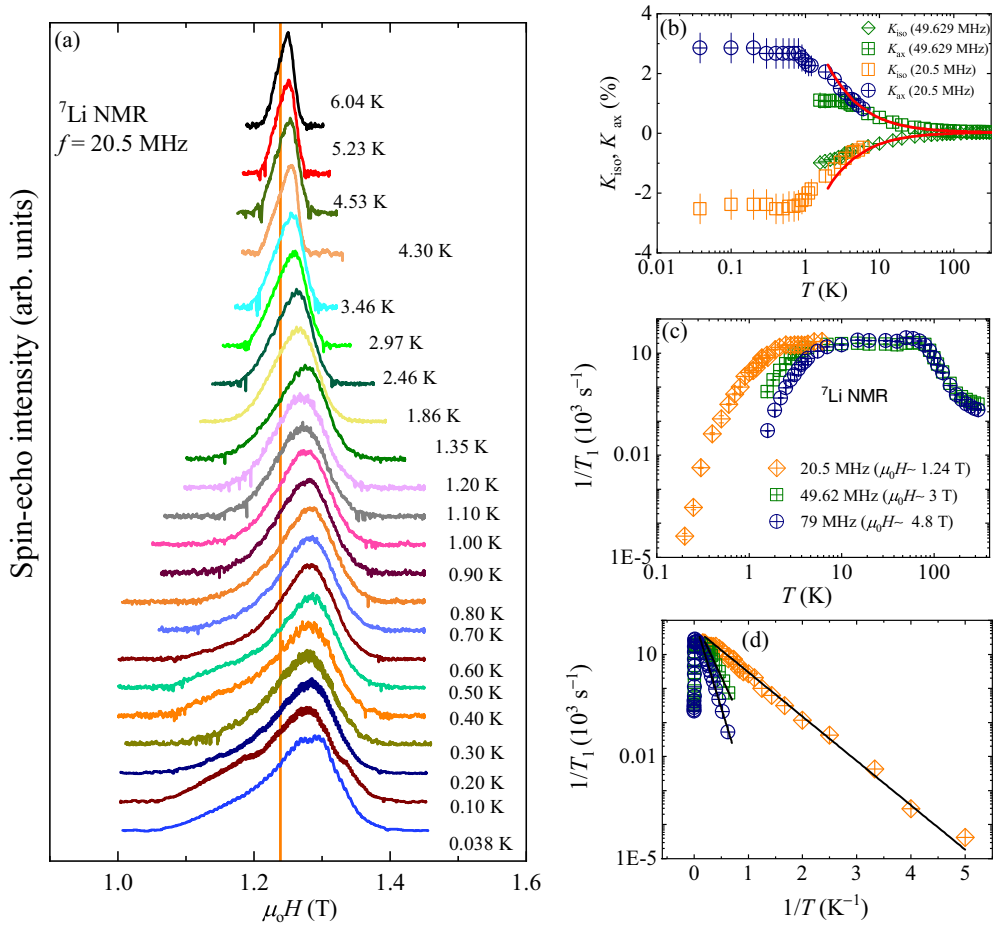

FIG. 4. ^{7}Li NMR spectra and spin-lattice relaxation rate in various magnetic fields reflecting the spin dynamics in the QSL state of LYTO. (a) ^{7}Li NMR spectra measured at constant frequency $\nu = 20.5$ MHz at a few representative temperatures. The orange vertical line corresponds to zero-shift reference line at 1.238 T. (b) The temperature dependence of isotropic (K_{iso}) and axial (K_{ax}) ^{7}Li NMR shifts of LYTO where the solid line is the scaled magnetic susceptibility measured in 1 T [53]. (c) The temperature dependence of the ^{7}Li NMR spin-lattice relaxation rate (T_1^{-1}) for three different fields in log-log scale. (d) T_1^{-1} as a function of inverse temperature (T^{-1}) for different fields in semilog scale. The black line represents a fit to a phenomenological model valid for thermally activated behavior of T_1^{-1} as discussed in the text. Error bars depict an uncertainty of one standard deviation.

Figure 5(f) shows Q-integrated energy cuts for different applied fields, which further reveal the presence of two humps whose center to center distance increases with fields. This spectrum is characteristic of an axially symmetric g tensor [67]. To further extract the values of the g tensor along the local anisotropy axis, $g_z = g_\parallel$, and in the perpendicular plane, $g_{xx} = g_{yy} = g_\perp$, we simulated the powder-averaged dynamical neutron structure factor [black lines in Fig. 5(f)] and found $g_\parallel = 4.0(1)$ and $g_\perp = 2.85(5)$, that account for all the data sets from 2 to 9 T. This leads to the powder-averaged value $g = \sqrt{g_\parallel^2/3 + 2g_\perp^2/3} = 3.27(7)$, which is in reasonable agreement with that obtained from other experiments. Given the presence of weak exchange interaction between Yb^{3+} moments, polarized neutron scattering experiments at ultralow temperature are desired to reveal dispersive spin fluctuations that is a hallmark of QSLs [24,39]. This is beyond the scope of the present paper, but provides a direction for further neutron scattering studies.

IV. SUMMARY

In the rare-earth-based quantum material $Li_3Yb_3Te_2O_{12}$ featuring a perfect hyperkagome lattice constituted by Yb^{3+} ions, our results using several complementary experimental techniques reveal that Yb^{3+} realizes a Kramers doublet and hence an effective $J_{eff} = 1/2$ degrees of freedom captures the essence of the low energy physics in the ground state. The Yb^{3+} spins remain dynamic, and is characterized by a quasielastic contribution in inelastic neutron scattering experiments and $J_{eff} = 1/2$ moments interacting with an energy of 0.6 K, which is rather low but typical for $4f$-based quantum materials. Furthermore, ac susceptibility data show no sign of spin freezing down to 45 mK. The lack of phase transition down to 54 mK is evidenced also by the magnetic specific heat data and a broad maximum around 0.18 K in ZF is attributed to the presence of short-range spin correlations. The compound thus presents an interesting setting wherein geometrical frustration conspires with quantum fluctuations

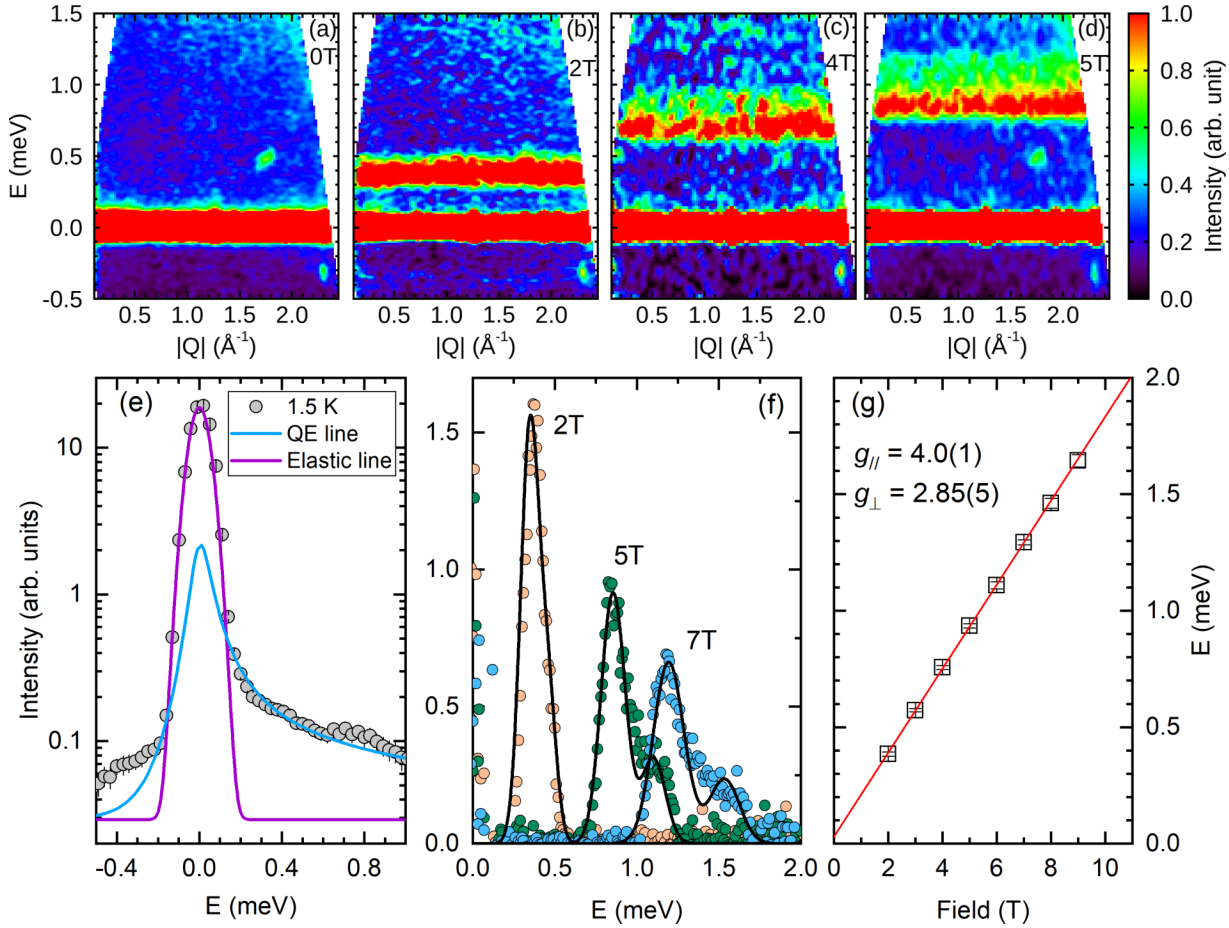

FIG. 5. Inelastic neutron scattering. (a)–(d) Intensity maps of the dynamical structure factor $S(Q, E)$ for polycrystalline LYTO measured at $T = 1.5$ K under zero applied field (a), $\mu_0 H = 2$ T (b), $\mu_0 H = 4$ T (c), and $\mu_0 H = 5$ T (d). (e), (f) Intensity versus energy for the Q-integrated region [0,1.5]Å^{-1} for the zero-field data set (e) and some selected data sets under applied fields (from which a field-independent background has been subtracted) (f). Experimental data points are symbols, purple line the estimated elastic contribution of the zero-field data, and blue line is the Lorentzian quasi-elastic contribution. Solid black lines in (f) are simulations assuming an axially symmetric g tensor (see text). (g) Median position of the spectrum as a function of the applied field (black squares). Red solid line is a linear fit.

to evade magnetic long-range ordering as further revealed by our NMR results down to 38 mK that is consistent with ac susceptibility and specific heat results, the primary hallmark of a dynamic ground state. A field-induced gap was evidenced in the specific heat, NMR relaxation rate, and neutron scattering results, which is reconciled with the Zeeman splitting of the effective spin $J_{\text{eff}} = 1/2$ of the Kramers doublet. The $4f$ moments on a hyperkagome lattice—an emblematic frustrated 3D model—offer a rare realization of a spin liquid. Our comprehensive results demonstrate a liquidlike dynamic state in a rare-earth hyperkagome, which might open the possibility of stabilizing a spin-orbit-driven quantum disordered state in $4f$ magnets. This family of rare-earth hyperkagome quantum material $Li_3RE_3Te_2O_{12}$ holds great potential to realize spin-orbit driven quantum phenomena and open avenues for modern theoretical approaches in establishing generic frameworks in the context of spin liquids.

ACKNOWLEDGMENTS

We acknowledge stimulating discussions with P. Mendels. P.K. acknowledges funding by the Science and Engineering Research Board and Department of Science and Technology, India through research grants. This research was supported by the U.S. Department of Energy, Office of Basic Energy Sciences, Division of Materials Sciences and Engineering. Ames Laboratory is operated for the U.S. Department of Energy by Iowa State University under Contract No. DE-AC02-07CH11358. E.K. and S.B. acknowledge the France Canada Research Fund for financial support. A.Z. acknowledges the financial support of the Slovenian Research agency under Program No. P1-0125 and Projects No. J1-2461 and No. N1-0148. A.M.S. thanks the URC/FRC of UJ and the SA-National Research Foundation (93549) for financial support.

[1] The rise of quantum materials, Nat. Phys. **12**, 105 (2016).

[2] Y. Tokura, M. Kawasaki, and N. Nagaosa, Emergent functions of quantum materials, Nat. Phys. **13**, 1056 (2017).

[3] D. N. Basov, R. D. Averitt, and D. Hsieh, Towards properties on demand in quantum materials, Nat. Mater. **16**, 1077 (2017).

[4] B. Keimer and J. E. Moore, The physics of quantum materials, Nat. Phys. **13**, 1045 (2017).

[5] P. W. Anderson, Resonating valence bonds: A new kind of insulator? Mater. Res. Bull. **8**, 153 (1973).

[6] L. Balents, Spin liquids in frustrated magnets, Nature (London) **464**, 199 (2010).

[7] M. J. P. Gingras and P. A. McClarty, Quantum spin ice: a search for gapless quantum spin liquids in pyrochlore magnets, Rep. Prog. Phys. **77**, 056501 (2014).

[8] H. Takagi, T. Takayama, G. Jackeli, G. Khaliullin, and S. E. Nagler, Concept and realization of Kitaev quantum spin liquids, Nat. Rev. Phys. **1**, 264 (2019).

[9] M. R. Norman, Colloquium: Herbertsmithite and the search for the quantum spin liquid, Rev. Mod. Phys. **88**, 041002 (2016).

[10] C. Nayak, S. H. Simon, A. Stern, M. Freedman, and S. Das Sarma, Non-Abelian anyons and topological quantum computation, Rev. Mod. Phys. **80**, 1083 (2008).

[11] L. Savary and L. Balents, Quantum spin liquids: A review, Rep. Prog. Phys. **80**, 016502 (2017).

[12] C. Broholm, R. J. Cava, S. A. Kivelson, D. G. Nocera, M. R. Norman, and T. Senthil, Quantum spin liquids, Science **367**, eaay0668 (2020).

[13] Y. Zhou, K. Kanoda, and T.-K. Ng, Quantum spin liquid states, Rev. Mod. Phys. **89**, 025003 (2017).

[14] M. Klanjšek, A. Zorko, R. Žitko, J. Mravlje, Z. Jagličić, P. K. Biswas, P. Prelovšek, D. Mihailovic, and D. Arčon, A high-temperature quantum spin liquid with polaron spins, Nat. Phys. **13**, 1130 (2017).

[15] Y. Li, D. Adroja, P. K. Biswas, P. J. Baker, Q. Zhang, J. Liu, A. A. Tsirlin, P. Gegenwart, and Q. Zhang, Muon Spin Relaxation Evidence for the U(1) Quantum Spin-Liquid Ground State in the Triangular Antiferromagnet $YbMgGaO_4$, Phys. Rev. Lett. **117**, 097201 (2016).

[16] P. Khuntia, M. Velazquez, Q. Barthélemy, F. Bert, E. Kermarrec, A. Legros, B. Bernu, L. Messio, A. Zorko, and P. Mendels, Gapless ground state in the archetypal quantum kagome antiferromagnet $ZnCu_3(OH)_6Cl_2$, Nat. Phys. **16**, 469 (2020).

[17] T.-H. Han, J. S. Helton, S. Chu, D. G. Nocera, J. A. Rodriguez-Rivera, C. Broholm, and Y. S. Lee, Fractionalized excitations in the spin-liquid state of a kagome-lattice antiferromagnet, Nature (London) **492**, 406 (2012).

[18] B. Bernu, C. Lhuillier, and L. Pierre, Signature of Néel Order in Exact Spectra of Quantum Antiferromagnets on Finite Lattices, Phys. Rev. Lett. **69**, 2590 (1992).

[19] Z. Zhu, P. A. Maksimov, S. R. White, and A. L. Chernyshev, Disorder-Induced Mimicry of a Spin Liquid in $YbMgGaO_4$, Phys. Rev. Lett. **119**, 157201 (2017).

[20] P. Khuntia, R. Kumar, A. V. Mahajan, M. Baenitz, and Y. Furukawa, Spin liquid state in the disordered triangular lattice $Sc_2Ga_2CuO_7$ revealed by NMR, Phys. Rev. B **93**, 140408(R) (2016).

[21] J. Knolle and R. Moessner, A field guide to spin liquids, Annu. Rev. Condens. Matter Phys. **10**, 451 (2019).

[22] P. Khuntia, F. Bert, P. Mendels, B. Koteswararao, A. V. Mahajan, M. Baenitz, F. C. Chou, C. Baines, A. Amato, and Y. Furukawa, Spin Liquid State in the 3D Frustrated Antiferromagnet $PbCuTe_2O_6$: NMR and Muon Spin Relaxation Studies, Phys. Rev. Lett. **116**, 107203 (2016).

[23] S. Chillal, Y. Iqbal, H. O. Jeschke, J. A. Rodriguez-Rivera, R. Bewley, P. Manuel, D. Khalyavin, P. Steffens, R. Thomale, A. T. M. N. Islam, J. Reuther, and B. Lake, Evidence for a three-dimensional quantum spin liquid in $PbCuTe_2O_6$, Nat. Commun. **11**, 2348 (2020).

[24] T. Arh, B. Sana, M. Pregelj, P. Khuntia, Z. Jagličić, M. D. Le, P. K. Biswas, P. Manuel, L. Mangin-Thro, A. Ozarowski, and A. Zorko, The Ising triangular-lattice antiferromagnet neodymium heptatantalate as a quantum spin liquid candidate, Nat. Mater. **21**, 416 (2022).

[25] W. Witczak-Krempa, G. Chen, Y. B. Kim, and L. Balents, Correlated quantum phenomena in the strong spin-orbit regime, Annu. Rev. Condens. Matter Phys. **5**, 57 (2014).

[26] P. A. Maksimov, Z. Zhu, S. R. White, and A. L. Chernyshev, Anisotropic-Exchange Magnets on a Triangular Lattice: Spin Waves, Accidental Degeneracies, and Dual Spin Liquids, Phys. Rev. X **9**, 021017 (2019).

[27] A. P. Ramirez, A. Hayashi, R. J. Cava, R. Siddharthan, and B. S. Shastry, Zero-point entropy in 'spin ice', Nature (London) **399**, 333 (1999).

[28] M. M. Bordelon, E. Kenney, C. Liu, T. Hogan, L. Posthuma, M. Kavand, Y. Lyu, M. Sherwin, N. P. Butch, C. Brown, M. J. Graf, L. Balents, and S. D. Wilson, Field-tunable quantum disordered ground state in the triangular-lattice antiferromagnet $NaYbO_2$, Nat. Phys. **15**, 1058 (2019).

[29] Y. Taguchi, Y. Oohara, H. Yoshizawa, N. Nagaosa, and Y. Tokura, Spin chirality, Berry phase, and anomalous Hall effect in a frustrated ferromagnet, Science **291**, 2573 (2001).

[30] Y. Machida, S. Nakatsuji, S. Onoda, T. Tayama, and T. Sakakibara, Time-reversal symmetry breaking and spontaneous Hall effect without magnetic dipole order, Nature (London) **463**, 210 (2010).

[31] G. Hester, H. S. Nair, T. Reeder, D. R. Yahne, T. N. DeLazzer, L. Berges, D. Ziat, J. R. Neilson, A. A. Aczel, G. Sala, J. A. Quilliam, and K. A. Ross, Novel Strongly Spin-Orbit Coupled Quantum Dimer Magnet: $Yb_2Si_2O_7$, Phys. Rev. Lett. **123**, 027201 (2019).

[32] P. Dalmas de Réotier, A. Yaouanc, P. C. M. Gubbens, C. T. Kaiser, C. Baines, and P. J. C. King, Absence of Magnetic Order in $Yb_3Ga_5O_{12}$: Relation Between Phase Transition and Entropy in Geometrically Frustrated Materials, Phys. Rev. Lett. **91**, 167201 (2003).

[33] H. J. Silverstein, K. Fritsch, F. Flicker, A. M. Hallas, J. S. Gardner, Y. Qiu, G. Ehlers, A. T. Savici, Z. Yamani, K. A. Ross, B. D. Gaulin, M. J. P. Gingras, J. A. M. Paddison, K. Foyevtsova, R. Valenti, F. Hawthorne, C. R. Wiebe, and H. D. Zhou, Liquidlike correlations in single-crystalline $Y_2Mo_2O_7$: An unconventional spin glass, Phys. Rev. B **89**, 054433 (2014).

[34] T. Fennell, P. P. Deen, A. R. Wildes, K. Schmalzl, D. Prabhakaran, A. T. Boothroyd, R. J. Aldus, D. F. McMorrow, and S. T. Bramwell, Magnetic Coulomb phase in the spin ice $Ho_2Ti_2O_7$, Science **326**, 415 (2009).

[35] S. Petit, E. Lhotel, B. Canals, M. Ciomaga Hatnean, J. Ollivier, H. Mutka, E. Ressouche, A. R. Wildes, M. R. Lees, and G. Balakrishnan, Observation of magnetic fragmentation in spin ice, Nat. Phys. **12**, 746 (2016).

[36] S. T. Bramwell and M. J. P. Gingras, Spin ice state in frustrated magnetic pyrochlore materials, Science **294**, 1495 (2001).

[37] B. Gao, T. Chen, D. W. Tam, C.-L. Huang, K. Sasmal, D. T. Adroja, F. Ye, H. Cao, G. Sala, M. B. Stone, C. Baines, J. A. T.

Verezhak, H. Hu, J.-H. Chung, X. Xu, S.-W. Cheong, M. Nallaiyan, S. Spagna, M. B. Maple, A. H. Nevidomskyy *et al.*, Experimental signatures of a three-dimensional quantum spin liquid in effective spin-1/2 $Ce_2Zr_2O_7$ pyrochlore, Nat. Phys. **15**, 1052 (2019).

[38] E. M. Smith, O. Benton, D. R. Yahne, B. Placke , R. Schfer , J. Gaudet, J. Dudemaine, A. Fitterman, J. Beare, A. R. Wildes, S. Bhattacharya , T. DeLazzer, C. R. C. Buhariwalla, N. P. Butch, R. Movshovich, J. D. Garrett, C. A. Marjerrison, J. P. Clancy, E. Kermarrec, G. M. Luke, A. D. Bianchi, K. A. Ross, and B. D. Gaulin, Case for a $U(1)_\pi$ Quantum Spin Liquid Ground State in the Dipole-Octupole Pyrochlore $Ce_2Zr_2O_7$, Phys. Rev. X **12**, 021015 (2022).

[39] R. Sibille, N. Gauthier, E. Lhotel, V. Porée, V. Pomjakushin, R. A. Ewings, T. G. Perring, J. Ollivier, A. Wildes, C. Ritter, T. C. Hansen, D. A. Keen, G. J. Nilsen, L. Keller, S. Petit, and T. Fennell, A quantum liquid of magnetic octupoles on the pyrochlore lattice, Nat. Phys. **16**, 546 (2020).

[40] J. A. M. Paddison, H. Jacobsen, O. A. Petrenko, M. T. Fernández-Díaz, P. P. Deen, and A. L. Goodwin, Hidden order in spin-liquid $Gd_3Ga_5O_{12}$, Science **350**, 179 (2015).

[41] L. O. Sandberg, R. Edberg, I.-M. B. Bakke, K. S. Pedersen, M. C. Hatnean, G. Balakrishnan, L. Mangin-Thro, A. Wildes, B. Fåk, G. Ehlers, G. Sala, P. Henelius, K. Lefmann, and P. P. Deen, Emergent magnetic behavior in the frustrated $Yb_3Ga_5O_{12}$ garnet, Phys. Rev. B **104**, 064425 (2021).

[42] Y. Cai, M. N. Wilson, J. Beare, C. Lygouras, G. Thomas, D. R. Yahne, K. Ross, K. M. Taddei, G. Sala, H. A. Dabkowska, A. A. Aczel, and G. M. Luke, Crystal fields and magnetic structure of the Ising antiferromagnet $Er_3Ga_5O_{12}$, Phys. Rev. B **100**, 184415 (2019).

[43] N. Zhao, H. Ge, L. Zhou, Z. M. Song, J. Yang, T. T. Li, L. Wang, Y. Fu, Y. F. Zhang, J. B. Xu, S. M. Wang, J. W. Mei, X. Tong, L. S. Wu, and J. M. Sheng, Antiferromagnetism and Ising ground states in the rare-earth garnet $Nd_3Ga_5O_{12}$, Phys. Rev. B **105**, 014441 (2022).

[44] D. G. Onn, H. Meyer, and J. P. Remeika, Calorimetric study of several rare-earth gallium garnets, Phys. Rev. **156**, 663 (1967).

[45] P. P. Deen, O. Florea, E. Lhotel, and H. Jacobsen, Updating the phase diagram of the archetypal frustrated magnet $Gd_3Ga_5O_{12}$, Phys. Rev. B **91**, 014419 (2015).

[46] R. Wawrzyńczak, B. Tomasello, P. Manuel, D. Khalyavin, M. D. Le, T. Guidi, A. Cervellino, T. Ziman, M. Boehm, G. J. Nilsen, and T. Fennell, Magnetic order and single-ion anisotropy in $Tb_3Ga_5O_{12}$, Phys. Rev. B **100**, 094442 (2019).

[47] X. G. Wen, F. Wilczek, and A. Zee, Chiral spin states and superconductivity, Phys. Rev. B **39**, 11413 (1989).

[48] R. Shindou, Nature of the possible magnetic phases in a frustrated hyperkagome iridate, Phys. Rev. B **93**, 094419 (2016).

[49] M. Hermele, M. P. A. Fisher, and L. Balents, Pyrochlore photons: The $u(1)$ spin liquid in a $s = \frac{1}{2}$ three-dimensional frustrated magnet, Phys. Rev. B **69**, 064404 (2004).

[50] S.-S. Gong, W. Zheng, M. Lee, Y.-M. Lu, and D. N. Sheng, Chiral spin liquid with spinon Fermi surfaces in the spin-$\frac{1}{2}$ triangular Heisenberg model, Phys. Rev. B **100**, 241111(R) (2019).

[51] F. A. Cevallos, S. Guo, and R. J. Cava, Magnetic properties of lithium-containing rare earth garnets $Li_3RE_3Te_2O_{12}$ (RE = Y, Pr, Nd, Sm-Lu), Mater. Res. Express **5**, 126106 (2018).

[52] B. H. Toby, EXPGUI, a graphical user interface for GSAS, J. Appl. Crystallogr. **34**, 210 (2001).

[53] See Supplemental Material at http://link.aps.org/supplemental/10.1103/PhysRevB.106.104404 for experimental details and results on magnetization, specific heat, and NMR.

[54] Y. Shimizu, H. Takeda, M. Tanaka, M. Itoh, S. Niitaka, and H. Takagi, An orbital-selective spin liquid in a frustrated heavy fermion spinel LiV_2O_4, Nat. Commun. **3**, 981 (2012).

[55] A. P. Dioguardi, S. Selter, U. Peeck, S. Aswartham, M.-I. Sturza, R. Murugesan, M. S. Eldeeb, L. Hozoi, B. Büchner, and H.-J. Grafe, Quasi-two-dimensional magnetic correlations in $Ni_2P_2S_6$ probed by ^{31}P NMR, Phys. Rev. B **102**, 064429 (2020).

[56] S. Toth and B. Lake, Linear spin wave theory for single-q incommensurate magnetic structures, J. Phys.: Condens. Matter **27**, 166002 (2015).

[57] R. Sibille, E. Lhotel, V. Pomjakushin, C. Baines, T. Fennell, and M. Kenzelmann, Candidate Quantum Spin Liquid in the Ce^{3+} Pyrochlore Stannate $Ce_2Sn_2O_7$, Phys. Rev. Lett. **115**, 097202 (2015).

[58] K. A. Ross, L. Savary, B. D. Gaulin, and L. Balents, Quantum Excitations in Quantum Spin Ice, Phys. Rev. X **1**, 021002 (2011).

[59] J. Xing, L. D. Sanjeewa, J. Kim, G. R. Stewart, M.-H. Du, F. A. Reboredo, R. Custelcean, and A. S. Sefat, Crystal synthesis and frustrated magnetism in triangular lattice $CsRESe_2$ (RE = La–Lu): Quantum spin liquid candidates $CsCeSe_2$ and $CsYbSe_2$, ACS Mater. Lett. **2**, 71 (2020).

[60] P. M. Sarte, K. Cruz-Kan, B. R. Ortiz, K. H. Hong, M. M. Bordelon, D. Reig-i Plessis, M. Lee, E. S. Choi, M. B. Stone, S. Calder, D. M. Pajerowski, L. Mangin-Thro, Y. Qiu, J. P. Attfield, S. D. Wilson, C. Stock, H. D. Zhou, A. M. Hallas, J. A. M. Paddison, A. A. Aczel *et al.*, Dynamical ground state in the XY pyrochlore Yb_2GaSbO_7, npj Quantum Mater. **6**, 42 (2021).

[61] R. Zhong, S. Guo, G. Xu, Z. Xu, and R. J. Cava, Strong quantum fluctuations in a quantum spin liquid candidate with a Co-based triangular lattice, Proc. Natl. Acad. Sci. **116**, 14505 (2019).

[62] A. Steppke, M. Brando, N. Oeschler, C. Krellner, C. Geibel, and F. Steglich, Nuclear contribution to the specific heat of $Yb(Rh_{0.93}Co_{0.07})_2Si_2$, Phys. Stat. Sol. B **247**, 737 (2010).

[63] Z.-F. Ding, Y.-X. Yang, J. Zhang, C. Tan, Z.-H. Zhu, G. Chen, and L. Shu, Possible gapless spin liquid in the rare-earth kagome lattice magnet $Tm_3Sb_3Zn_2O_{14}$, Phys. Rev. B **98**, 174404 (2018).

[64] P. D. de Réotier and A. Yaouanc, Muon spin rotation and relaxation in magnetic materials, J. Phys.: Condens. Matter **9**, 9113 (1997).

[65] K. Y. Zeng, L. Ma, Y. X. Gao, Z. M. Tian, L. S. Ling, and L. Pi, NMR study of the spin excitations in the frustrated antiferromagnet $Yb(BaBO_3)_3$ with a triangular lattice, Phys. Rev. B **102**, 045149 (2020).

[66] J. A. Quilliam, F. Bert, E. Kermarrec, C. Payen, C. Guillot-Deudon, P. Bonville, C. Baines, H. Luetkens, and P. Mendels, Singlet Ground State of the Quantum Antiferromagnet $Ba_3CuSb_2O_9$, Phys. Rev. Lett. **109**, 117203 (2012).

[67] A. Abragam and B. Bleaney, *Electron Paramagnetic Resonance of Transition Ions* (Oxford University Press, Oxford, 2012)